σ–σ and σ–π pnicogen bonds in complexes H2XP:PCX, for X = F, Cl, OH, NC, CN, CCH, CH3, and H

ARTICLE *in* THEORETICAL CHEMISTRY ACCOUNTS · APRIL 2014

Impact Factor: 2.23 · DOI: 10.1007/s00214-014-1464-y

3 AUTHORS, INCLUDING:

Ibon Alkorta
Spanish National Research Council
679 PUBLICATIONS **12,371** CITATIONS
SEE PROFILE

José Elguero
Spanish National Research Council
1,502 PUBLICATIONS **22,122** CITATIONS
SEE PROFILE

Theor Chem Acc (2014) 133:1464
DOI 10.1007/s00214-014-1464-y

REGULAR ARTICLE

σ–σ and σ–π pnicogen bonds in complexes H_2XP:PCX, for X = F, Cl, OH, NC, CN, CCH, CH_3, and H

Janet E. Del Bene · Ibon Alkorta · José Elguero

Received: 21 November 2013 / Accepted: 11 February 2014

Abstract Ab initio MP2/aug'-cc-pVTZ calculations have been carried out on complexes H_2XP_s:P_tCX, for X = F, Cl, OH, NC, CN, CCH, CH_3, and H, in search of complexes stabilized by P···P pnicogen bonds. These intermolecular bonds arise when a pnicogen atom acts as a Lewis acid for complex formation. Three sets of equilibrium structures have been found on the H_2XP_s:P_tCX potential surfaces. Conformation A complexes have P···P σ–σ pnicogen bonds, which involve the σ systems of both P atoms. Conformations B and C are stabilized by σ–π pnicogen bonds, which involve the σ system of H_2XP and the π system of PCX. Binding energies of B and C complexes are similar and are greater than the binding energies of the A conformers. Charge transfer stabilizes A, B, and C conformers. In A complexes, the dominant charge transfer is from the lone pair of PCX to the antibonding σ*P–A orbital of PH_2X, with A the atom of X directly bonded to P. For conformations B and C, the dominant charge transfer is from the P=C π orbital to the σ*P–A orbital of H_2XP. Although the binding energies of these complexes do not correlate with the intermolecular P–P distances, both the charge-transfer energies and the equation-of-motion coupled cluster singles and doubles one-bond ^{31}P–^{31}P spin–spin coupling constants do correlate with the P–P distances. The largest coupling constants $^{1p}J(P–P)$ are found for complexes with conformation A, due to the nature of the σ–σ pnicogen bond and the dominance of the Fermi contact term. For a given X, $^{1p}J(P–P)$ values are ordered A > C > B.

Keywords Structures and binding energies · Intermolecular interactions · σ–σ and σ–π pnicogen bonds · Charge-transfer energies · ^{31}P–^{31}P EOM-CCSD spin–spin coupling constants $^{1p}J(P–P)$

1 Introduction

Subsequent to the landmark 2011 paper of Hey-Hawkins et al. [1], there have been many papers published on the subject of intermolecular interactions through the formation of pnicogen bonds [2–32]. This bond arises when a pnicogen atom (N, P, As) acts as a Lewis acid by accepting a pair of electrons from a Lewis base. When two pnicogen atoms participate in forming a bond, each acts as both an electron-pair acceptor and an electron-pair donor. Most studies of pnicogen bonds have involved the PH_3 molecule and its derivatives.

Recently, we asked to what extent a formally sp^2-hybridized P atom could participate in a P···P pnicogen bond in complexes $(H_2C=PX)_2$ and $H_2C=(X)P:PXH_2$ for a variety of substituents X [30, 32]. In the latter study, we identified a series of complexes stabilized by pnicogen bonds, which involve π electron donation by $H_2C=PX$ to PH_2X through the σ-hole, and donation of the lone pair of

Dedicated to the memory of Professor Isaiah Shavitt and published as part of the special collection of articles celebrating his many contributions.

Electronic supplementary material The online version of this article (doi:10.1007/s00214-014-1464-y) contains supplementary material, which is available to authorized users.

J. E. Del Bene (✉)
Department of Chemistry, Youngstown State University, Youngstown, OH 44555, USA
e-mail: jedelbene@ysu.edu

I. Alkorta (✉) · J. Elguero
Instituto de Química Médica (IQM–CSIC), Juan de la Cierva, 28006 Madrid, Spain
e-mail: ibon@iqm.csic.es

Published online: 05 March 2014

PH_2X to $H_2C{=}PX$ through the π-hole. To our knowledge, this was the first time that pnicogen-bonded complexes with a π electron donor and π-hole acceptor involving the same π bond had been reported. We referred to this bond as a π–σ pnicogen bond to indicate that it is the π system of one molecule and the σ system of the other that interact. It should be noted, however, that pnicogen bonds involving π-electron donors or π-hole acceptors have been discussed previously in the literature, but the π-donors and π-hole acceptors are not the same π bond [7, 21, 29, 33, 34].

Since PH_2X can form stable σ–π pnicogen-bonded complexes with $H_2C{=}(X)P$, we decided to investigate a related series of complexes in which PH_2X interacts with PCX, searching for both σ–π and σ–σ pnicogen bonds. This study yielded three different conformations of complexes $H_2XP{:}PCX$, for X = F, Cl, OH, NC, CN, CCH, CH_3, and H. In this paper, we report the equilibrium structures of these complexes, their binding energies, bonding properties, and ^{31}P–^{31}P spin–spin coupling constants.

2 Methods

The structures of the isolated monomers and the complexes $H_2XP{:}PCX$ were optimized at second-order Møller-Plesset perturbation theory (MP2) [35–38] with the aug'-cc-pVTZ basis set [39]. This basis set is derived from the Dunning aug-cc-pVTZ basis set [40, 41] by removing diffuse functions from H atoms. Frequencies were computed to establish that the optimized structures correspond to equilibrium structures on their potential surfaces. In addition, we determined transition structures which are the barriers to the interconversion of the B and C conformers of $H_2FP{:}PCF$ and $H_3P{:}PCH$. Optimization and frequency calculations were performed using the Gaussian 09 program [42].

The electron densities of these complexes have been analyzed using the atoms in molecules (AIM) methodology [43–46] and the electron localization function (ELF) [47] employing the AIMAll [48] and Topmod [49] programs. The topological analysis of the electron density produces the molecular graph of each complex. This graph identifies the location of electron density features of interest, including the electron density (ρ) maxima associated with the various nuclei, saddle points which correspond to bond critical points (BCPs), and ring critical points which indicate a minimum electron density within a ring. The zero gradient line which connects a BCP with two nuclei is the bond path. The ELF function illustrates those regions of space at which the electron density is high. MP2/aug'-cc-pVTZ atomic and molecular charges have been obtained using the natural bond orbital (NBO) method [50]. The stabilizing charge-transfer interactions in these binary complexes have been computed using the NBO-6 program [51].

Spin–spin coupling constants were evaluated using the equation-of-motion coupled cluster singles and doubles (EOM-CCSD) method in the CI (configuration interaction)-like approximation [52, 53], with all electrons correlated. For these calculations, the Ahlrichs [54] qzp basis set was placed on ^{13}C, ^{15}N, ^{17}O, and ^{19}F, and the qz2p basis set on ^{31}P and ^{35}Cl. The Dunning cc-pVDZ basis set was placed on all ^{1}H atoms. Only $^{1p}J(P–P)$ coupling constants are reported in this paper. The EOM-CCSD calculations were performed using ACES II [55] on the IBM Cluster 1350 (Glenn) at the Ohio Supercomputer Center.

3 Results and discussion

In order to differentiate the two P atoms, we will refer to them as P_s, the P atom that forms single covalent bonds in P_sH_2X, and P_t for the triply bonded P in P_tCX. Although many minima may exist on the $H_2XP_s{:}P_tCX$ surfaces, we have restricted our searches to regions that have structural characteristics associated previously with complexes stabilized by pnicogen bonds. We began by searching the region in which the interaction involves the formation of a σ–σ pnicogen bond. In the resulting conformation A complexes, $A–P_s\cdots P_t–C$ approaches linearity, with A being the atom of X directly bonded to P_s, and C the carbon of PCX. We then investigated regions in which PCX interacts through its π-electron system with PXH_2 to form σ–π bonds. In conformation B complexes, a σ–π pnicogen bond forms in which $A–P_s\cdots C$ approaches linearity. In conformation C, the σ–π pnicogen bond has $A–P_s\cdots P_t$ approaching linearity. These three conformations are illustrated in Fig. 1. We did not search regions in which one H of PH_2X

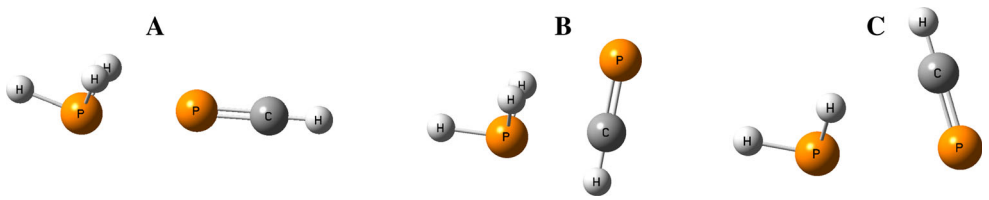

Fig. 1 $H_3P{:}PCH$ complexes with conformations **A**, **B**, and **C**. All complexes have C_s symmetry except for $H_2(CN)P{:}PCCN$ and $H_2(CCH)P{:}PCCCH$ B which have C_1 symmetry

assumes a linear arrangement, since $(PH_2X)_2$ complexes with H–P···P–A linear have significantly reduced binding energies relative to the same complexes with A–P···P–A linear [18, 23].

The binding energies of conformation A, B, and C complexes are reported in Table 1. These are ordered according to decreasing binding energies of conformation C. All substituents X form B and C complexes stabilized by σ–π bonds. Conformation A complexes have P···P σ–σ pnicogen bonds and are formed by all molecules except those containing the more electronegative substituents F and Cl. H_2(OH)P:PCOH is a planar complex, but it has not been included in this study since it is stabilized primarily by an O–H···P_s hydrogen bond. Its binding energy of −34.2 kJ/mol is significantly greater than the binding energies of the pnicogen-bonded complexes.

3.1 Conformation A complexes

The structures, total energies, and bond paths connecting the two P atoms of conformation A complexes are reported in Table S1 of the Electronic Supporting Material. Table 2 reports the binding energies, P–P distances, and the angles P_t–P_s–A and P_s–P_t–C in these complexes. Of the three conformations, the A complexes are the most weakly bound, with binding energies ranging from −3.1 kJ/mol for H_2(CN)P:PCCN to −7.4 kJ/mol for H_2(CCH)P:PCCCH. Moreover, these binding energies are lower than the binding energies of the corresponding complexes $(PH_2X)_2$ and H_2C=(X)P:PXH_2. For a given X, the intermolecular P–P distances in A conformers decrease in the order H_2-XP:PCX > H_2C=(X)P:PXH_2 > $(PH_2X)_2$. As noted previously for complexes with σ–σ pnicogen bonds, A–P···P–A' arrangements tend to approach linearity. The P_s–P_t–C alignment in conformation A complexes closely approaches linearity, with the P_s–P_t–C angle varying between 175 and 179°. The P_t–P_s–A angle deviates to some extent from linearity, with values between 158 and 167°.

Complexes with pnicogen bonds are stabilized by charge transfer. The more favorable charge-transfer interaction involves donation of the P_t lone pair of PCX to the σ*P–A orbital of PH_2X. Charge-transfer energies range from 3.4 kJ/mol for X = CH_3 to 9.4 kJ/mol when X = NC. In contrast, charge transfer from the P_s lone pair of PH_2X to the σ*P=C orbital of PCX is 2.5 kJ/mol when X = NC, and 1.4 or 1.5 kJ/mol for the remaining complexes. The preference for charge transfer from H_2C=PX to PH_2X was observed previously in conformation A complexes [32]. The P_t(lp) → σ*P–A charge-transfer energies do not correlate with the binding energies of these complexes, but do correlate with the P–P distances, as can be seen in Fig. 2. The data of Table 3 also indicate that the PH_2X molecules become slightly negatively charged in the complexes, except for $P(CH_3)H_2$ which is uncharged. Both P_s and P_t are positively charged in the monomers, and that positive charge is reduced upon complexation. The positive charge on P_s in conformation A complexes varies from 0.043e in H_3P:PCH to 0.576e in H_2(NC)P:PCNC. The positive charge on P_s decreases in the order:

Table 1 Binding energies (ΔE, kJ/mol) of complexes H_2XP:PCX with conformations A, B, and C

H_2XP:PCX, X =	ΔE(A)	ΔE(B)	ΔE(C)
Cl		−16.4	−17.6
F		−16.6	−15.6
CCH	−7.4	−13.3	−14.7
OH[a]	[a]	−13.2	−14.2
NC	−4.2	−12.0	−13.5
CN	−3.1	−9.6	−10.6
CH_3	−5.7	−12.6	−10.0
H	−4.7	−8.7	−7.5

Ordered according to decreasing binding energy of conformation C complexes

[a] This complex is stabilized primarily by an O–H···P_s hydrogen bond, with a binding energy of −34.2 kJ/mol

Table 2 Binding energies (ΔE, kJ/mol), P–P distances (R, Å), and P_t–P_s–A and P_s–P_t–C angles (<, deg) for conformation A complexes

H_2XP:PCX, X =	ΔE	R(P–P)	<P_t–P_s–A	<P_s–P_t–C
CCH	−7.4	3.594	163	179
NC	−4.2	3.521	166	179
CN	−3.1	3.649	167	176
CH_3	−5.7	3.705	160	176
H	−4.7	3.772	158	175

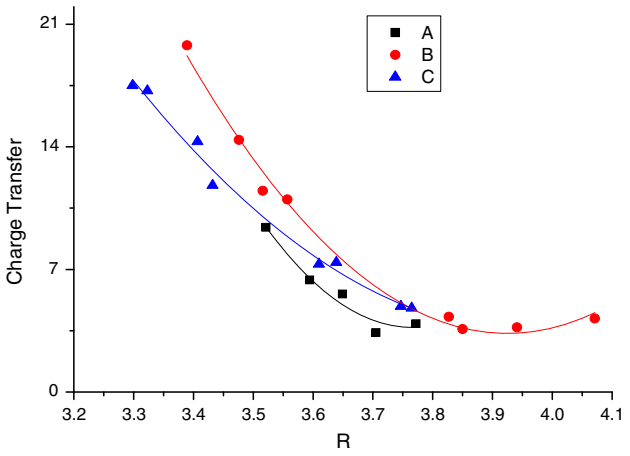

Fig. 2 Charge-transfer energies from PCX to PH_2X (kJ/mol) versus the P–P distance (R, Å) for conformation *A*, *B*, and *C* complexes. Correlation coefficients R^2 are 0.963, 0.992, and 0.990, respectively

Table 3 Charges on PH_2X, changes in the charges on the P atoms (δe, au), and charge-transfer energies (kJ/mol) for conformation A complexes $H_2XP_s{:}P_tCX$

H_2XP:PCX, X =	Charge on PH_2X	$\delta e(P_s)$[a]	$\delta e(P_t)$[a]	$P_t(lp) \rightarrow \sigma^*P_s$–A	$P_s(lp) \rightarrow \sigma^*P_t$=C
CCH	−0.003	−0.011	−0.014	6.4	1.4
NC	−0.006	−0.017	–0.033	9.4	2.5
CN	−0.003	−0.016	−0.028	5.6	1.5
CH_3	0.000	−0.003	−0.003	3.4	1.5
H	−0.001	−0.005	−0.007	3.9	1.4

[a] Both P_s and P_t are positively charged in the isolated monomers

Table 4 Binding energies (ΔE, kJ/mol), P–P and P_s–C distances (R, Å), and C–P_s–A angles (< , deg) for conformation B complexes

H_2XP:PCH, X =	ΔE	R(P–P)	R(P_s–C)	<C–P_s–A
Cl	−16.4	3.476	3.326	175
F	−16.6	3.389	3.070	172
CCH	−13.3	3.827	3.404	161
OH	−13.2	3.516	3.251	175
NC	−12.0	3.557	3.241	177
CN	−9.6	3.941	3.426	165
CH_3	−12.6	3.850	3.439	177
H	−8.7	4.071	3.413	171

These complexes have C_s symmetry, except for H_2(CN)P:PCCN and H_2(CCH)P:PCCCH which have C_1 symmetry

$$NC \approx CN > CCH > H > CH_3.$$

The positive charge on P_t varies from 0.479e in $H_2(CH_3)$-P:$PCCH_3$ to 0.617e in H_2(CN)P:PCCN and decreases in a similar order:

$$NC > CN > CCH > H > CH_3.$$

For complexes with X = NC, CN, and CCH, the decrease in the positive charge on P_t is noticeably greater than the decrease in the positive charge on P_s.

3.2 Conformation B complexes

The structures, total energies, and bond paths of conformation B complexes are given in Table S1 of the Electronic Supporting Material. These bond paths connect P_s with PCX through the π system at the P≡C C atom. The classification as conformation B is based on the C–P_s–A angles which range from 161 to 177° and are closer to linearity than the corresponding P_t–P_s–A angles. Conformation B pnicogen bonds are σ–π bonds, which involve the σ system of PH_2X and the P≡C π bond. The binding energies, P–P and P_s–C distances, and C–P_s–A angles are reported in Table 4. The binding energies of these complexes range from −8.7 kJ/mol for H_3P:PCH to –16.6 kJ/mol for H_2FP:PCF. The ordering is consistent with the ordering of conformation C complexes, except for $H_2(CH_3)$P:$PCCH_3$, which has a noticeably higher binding energy than its C counterpart. The P_s–C distances are always shorter than the corresponding P–P distances, but once again, there is no correlation between the binding energies and either the P–P or the P_s–C intermolecular distances. Both linear and quadratic trendlines have correlation coefficients R^2 of 0.73.

Conformation B complexes are also stabilized by charge-transfer interactions. Since the P≡C bond is polarized toward C, charge transfer occurs from the π bond at C through the σ-hole to P_s, and from the lone pair on P_s to P_t through the π hole. In all complexes but one, the dominant charge transfer is from the πP=C orbital of PCX to the σ*P–A antibonding orbital of PH_2X, as can be seen from the data of Table 5. The single exception is X = H, for which charge transfer from the πP=C orbital of PCH to the σ*P–H orbital is 0.2 kJ/mol less stabilizing. Having the C–P_s–A angle approach linearity is favorable for charge transfer from PCX to PH_2X. In addition, the P_s–P_t–C angles are acute, ranging from 55 to 68°, thereby leading to shorter distances between P_s and C, and facilitating charge transfer from the P=C π bond, which is polarized toward C. The πP=C→σ*P–A charge-transfer energies vary from 3.6 kJ/mol for X = CH_3 to 19.8 kJ/mol for X = F. Charge-transfer energies from the lone pair on P_s to the π*P=C orbital range from 1.3 kJ/mol for X = CCH to 10.0 kJ/mol for X = F. The πP=C→σ*P–A charge-transfer energies do not correlate with the binding energies of conformation B complexes or with the P_s–C distances, but do correlate with the intermolecular P–P distances, as shown in Fig. 2. The net result of charge transfer is to produce a slightly negatively charged PH_2X molecule, except for PH_2CH_3 and PH_3, and to reduce the positive charge on P_s. The positive charge on P_t may increase or decrease, as seen from the data of Table 5. Figure 3 illustrates the regions of high electron density involved in charge transfer in H_2FP:PCF conformation B.

3.3 Conformation C complexes

Table S1 of the Electronic Supporting Material reports the structures, total energies, and molecular graphs for

Table 5 Charges on PH_2X, changes in the charges on the P atoms (δe, au), and charge-transfer energies (kJ/mol) for conformation B complexes $H_2XP_s{:}P_t{\equiv}CX$

H_2XP:PCX, X =	Charge on PH_2X	δe(P_s)	δe(P_t)	πP=C → σ*P_s–A	P_s(lp) → π*P=C
Cl	−0.011	−0.017	−0.003	14.4	5.1
F	−0.005	−0.020	0.006	19.8	10.0
CCH	−0.003	−0.005	0.005	4.3	1.3
OH	−0.002	−0.007	−0.002	11.5	5.1
NC	−0.007	−0.014	−0.002	11.0	5.6
CN	−0.003	−0.010	0.014	3.7	1.5
CH_3	0.003	−0.011	−0.010	3.6	3.4
H	0.002	−0.008	−0.002	4.2	4.4

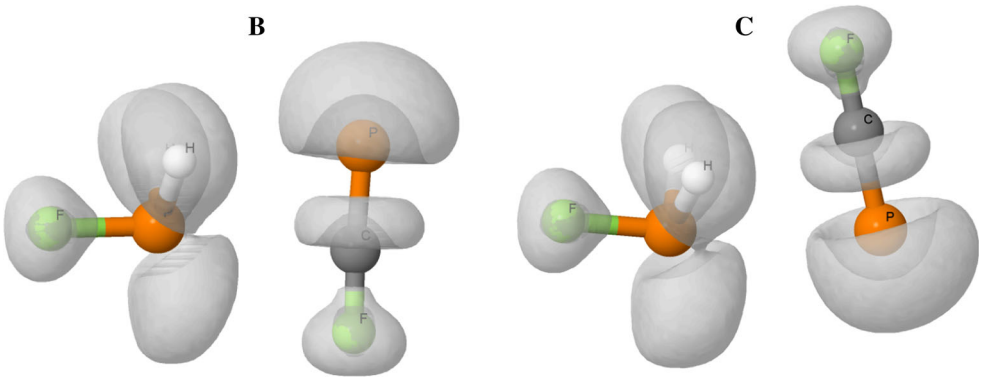

Fig. 3 The ELF representations of the regions of high electron density in H_2FP:PCF B and C

Table 6 Binding energies (ΔE, kJ/mol), P–P and P–C distances (R, Å), and P_t–P_s–A angles (<, deg) for conformation C complexes

H_2XP:PCH, X =	ΔE	R(P–P)	R(P_s–C)	<P_t–P_s–A
Cl	−17.6	3.323	3.313	174
F	−15.6	3.298	3.270	175
CCH	−14.7	3.610	3.431	172
OH	−14.2	3.432	3.360	171
NC	−13.5	3.407	3.317	175
CN	−10.6	3.639	3.428	176
CH_3	−10.0	3.747	3.571	166
H	−7.5	3.765	3.702	168

conformation C complexes. The bond paths connect P_s to the π system of PCX, usually but not always at P_t. These complexes are differentiated from the conformation B complexes in so far as the P_t–P_s–A angles approach closer to linearity than the corresponding C–P_s–A angles. The values of the P_t–P_s–A angles are reported in Table 6 and can be seen to vary between 166 and 176°. Table 6 also shows that the P_s–C distances are still shorter than the P–P distances, although the difference between them is much less than found for conformation B complexes due to the values of the P_s–P_t–C angles. These angles vary between 70 and 76°, and are therefore larger than the corresponding angles in conformation B.

Table 6 also reports the binding energies of conformation C complexes. These energies range from −7.5 kJ/mol for X = H to −17.6 kJ/mol for X = Cl. Conformation C complexes are more stable than conformation B for 5 of 8 complexes, but the binding energies of B and C are similar, differing by 1 to 1.5 kJ/mol. The single exception is conformation C of $H_2(CH_3)P{:}PCCH_3$, which is 2.5 kJ/mol less stable than B. The binding energies do not correlate with the P–P distances.

Figure 3 illustrates the regions of high electron density in H_2FP:PCF conformation C. The regions associated with the lone pair on P_s and the P=C π bond give rise to the charge-transfer interactions. A charge-transfer pattern similar to that observed for conformation B complexes is found for conformation C. Charge transfer involves electron donation by πP=C to the σ*P_s–A antibonding orbital through the σ-hole at P_s, and lone-pair donation by P_s to the π*P=C orbital through the π-hole at P_t. As can be seen from the data of Table 7, the πP=C→σ*P_s–A charge-transfer energies are significantly greater than the P_s(lp) → π*P=C energies and are also greater than the corresponding πP=C→σ*P_s–A energies of conformation B complexes, except for H_2FP:PCF which has the largest charge-transfer energy among all complexes. Once again, the πP=C→σ*P_s–A charge-transfer energies correlate with the P–P distances, as seen in Fig. 2. The net result of charge transfer is to make PH_2X negatively charged in the

Table 7 Charges on PH_2X, changes in the charges on the P atoms (δe, au), and charge-transfer energies (kJ/mol) for conformation C complexes $H_2XP_s{:}P_t{\equiv}CX$

H_2XP:PCX, X =	Charge on PH_2X	$\delta e(P_s)$	$\delta e(P_t)$	$\pi P{=}C \rightarrow \sigma^* P_s{-}A$	$P_s(lp) \rightarrow \pi^* P{=}C$
Cl	−0.018	−0.019	0.020	17.2	5.1
F	−0.012	−0.017	0.025	17.5	6.2
CCH	−0.004	−0.013	0.018	7.3	1.0
OH	−0.007	−0.010	0.019	11.8	4.1
NC	−0.012	−0.023	0.021	14.3	2.7
CN	−0.005	−0.023	0.022	7.4	0.7
CH_3	−0.002	0.010	0.015	4.9	0.9
H	−0.003	−0.004	0.012	4.8	1.5

Table 8 Intermolecular P–P distances (R, Å) and $^{31}P{-}^{31}P$ spin–spin coupling constants (Hz) for H_2XP:PCX complexes with conformations A, B, and C

H_2XP:PCX	A		B		C	
	R(P–P)	$^{1p}J(P{-}P)$	R(P–P)	$^{1p}J(P{-}P)$	R(P–P)	$^{1p}J(P{-}P)$
X = Cl			3.476	41.1	3.323	116.7
F			3.389	54.3	3.298	119.7
CCH	3.594	157.6	3.827	16.9	3.610	49.4
OH			3.516	41.9	3.432	83.3
NC	3.521	209.4	3.557	31.9	3.407	86.8
CN	3.649	150.4	3.941	14.9	3.639	48.0
CH_3	3.705	100.8	3.850	11.9	3.747	32.6
H	3.772	88.3	4.071	7.3	3.765	34.5

complex, decrease the positive charge on P_s, and increase the positive charge on P_t.

B and C complexes are energetically and structurally similar, since both are stabilized by pnicogen bonds involving P_s of PH_2X and the PCX π system. What is the barrier for interconversion of these conformers? To answer this question, we have optimized transition structures on the H_3P:PCH and H_2FP:PCF surfaces. These structures have C_1 symmetry, with the PCH and PCF molecules nearly perpendicular to the PH_3 and PH_2F symmetry planes, respectively. The structures suggest that B and C are interconverted by rotation of the PCH or PCF molecules about an axis which connects P_s to the P=C π bond, and by accompanying changes in the P_s–C and P–P bond lengths. For H_3P:PCH, the P_s–C bond length in the transition structure is similar to that in C, while the P–P bond length increases. Both P_s–C and P–P bonds are longer in the H_2FP:PCF transition structure that they are in both B and C. The interconversion of B and C via rotation indicates that these complexes remain intact in the transition state, with similar binding energies of –6.1 and –6.9 kJ/mol, respectively. Relative to the less stable conformer C, the barriers to converting C to B are 2.6 and 9.7 kJ/mol for H_3P:PCH and H_2FP:PCF, respectively.

3.4 $^{31}P{-}^{31}P$ spin–spin coupling constants

$^{31}P{-}^{31}P$ spin–spin coupling constants across pnicogen bonds have been computed for complexes with conformations A, B, and C. Table S2 of the Electronic Supporting Material reports components of $^{1p}J(P{-}P)$. Although previous investigations of $^{31}P{-}^{31}P$ coupling across pnicogen bonds suggest that the Fermi contact term is an excellent approximation to total $^{1p}J(P{-}P)$, we computed all terms, the paramagnetic spin orbit (PSO), diamagnetic spin orbit (DSO), Fermi contact (FC), and spin dipole (SD) terms for 12 H_2XP:PCX complexes. The largest differences between the FC terms and total $^{1p}J(P{-}P)$ are found for complexes in which X is one of the more electronegative substituents, namely F, Cl, and OH. For these, the difference between the FC term and $^{1p}J(P{-}P)$ ranges from 2.0 to 5.8 Hz and arises primarily from the contribution of the PSO term. For the remaining 9 complexes with C_s symmetry, PSO, DSO, and FC terms were computed. The largest PSO contribution is 1.5 Hz for X = NC, with the PSO terms for the remaining complexes having absolute values less than 0.7 Hz. For the two conformation B complexes of C_1 symmetry with X = CCH and CN, only the FC terms were evaluated due to computational expense. This can be justified by noting that the PSO terms for the A and C complexes with these same substituents have absolute values no greater than 0.1 Hz. In Table 8, total $^{1p}J(P{-}P)$ values are reported for 12 complexes, and the FC terms have been used to approximate $^{1p}J(P{-}P)$ for the remaining complexes.

Table 8 reports the P–P distances and values of $^{1p}J(P{-}P)$ for complexes H_2XP:PCX with conformations A, B, and C. For a given substituent X, the order of decreasing $^{1p}J(P{-}P)$

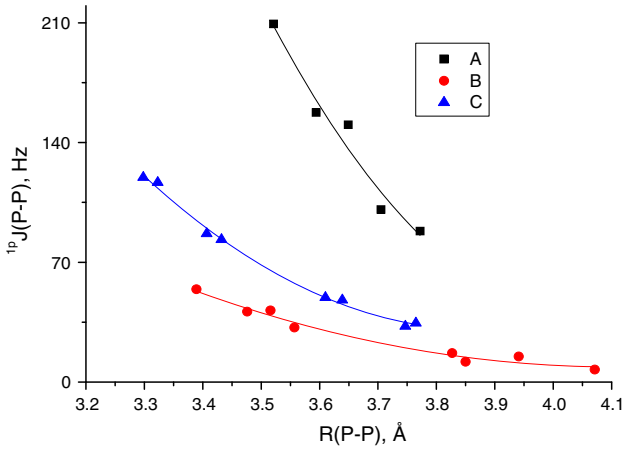

Fig. 4 ^{1p}J(P–P) versus the P–P distance for complexes with conformations *A*, *B*, and *C*

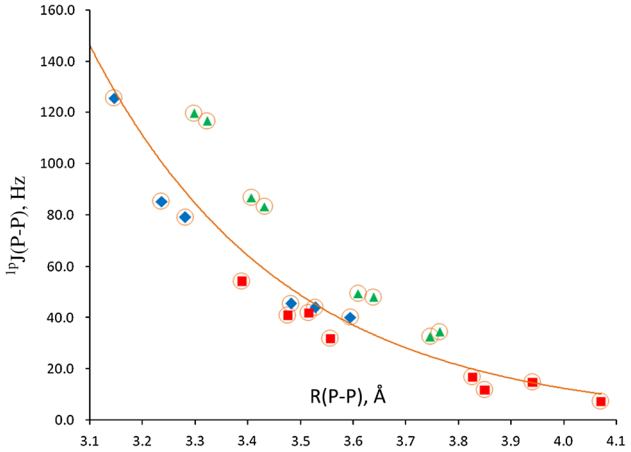

Fig. 5 Coupling constants ^{1p}J(P–P) versus the P–P distances for σ–π pnicogen bonds in H_2XP:PCX conformations B (*red square*) and C (*green triangle*) and H_2C=(X)P:PXH_2 conformation C (*blue diamond*). The symbol *circle* includes all complexes for which the best-fit trendline is an exponential

is A > C > B. The large values of ^{1p}J(P–P) for conformation A complexes may be attributed primarily to the nature of the pnicogen bond, which is a σ–σ bond, and the dependence of the dominant FC term on s-electron densities in both ground and excited states. The nature of the FC term is also consistent with the reduced values of ^{1p}J(P–P) for conformations B and C, since they are stabilized by σ–π pnicogen bonds which involve the π electrons of PCX. That ^{1p}J(P–P) for a given X is greater for the conformation C complex is consistent with the shorter P–P distances in C, and with the A–P_s–P_t arrangement which approaches linearity. Figure 4 presents plots of ^{1p}J(P–P) versus the P–P distance for complexes with conformations A, B, and C. The good correlation between these two variables is evident, with the second-order trendlines having correlation coefficients R^2 of 0.961, 0.995, and 0.976, respectively.

In a previous study, we compared coupling constants ^{1p}J(P–P) for conformation A complexes $(PH_2X)_2$, H_2C=(X)P:PXH_2, and $(H_2C{=}PX)_2$ with σ–σ pnicogen bonds. We can now compare ^{1p}J(P–P) for the σ–π pnicogen bonds in conformations B and C of H_2XP:PCX with ^{1p}J(P–P) σ–π bonds for conformation C complexes of H_2C=(X)P:PXH_2. That comparison is illustrated in Fig. 5. The exponential trendline for the entire set of points has a correlation coefficient of 0.859. However, it is apparent from Fig. 5 that all of the points for conformation C complexes of H_2XP:PCX with A–P_s···P_t approaching linearity lie above the trendline and have larger values of ^{1p}J(P–P) at each P–P distance. Values for H_2XP:PCX conformation B with A–P_s···C linear and conformation C of H_2C=(X)P_d:P_sXH_2 with A–P_s···P_d linear lie either on or below the trendline, and have similar values at similar distances. The exponential trendline for ^{1p}J(P–P) versus R(P–P) for these two sets treated together has a correlation coefficient R^2 of 0.958.

4 Conclusions

Ab initio MP2/aug'-cc-pVTZ calculations have been carried out on a series of complexes H_2XP:PCX, for X = F, Cl, OH, NC, CN, CCH, CH_3, and H, to identify and characterize σ–σ and σ–π pnicogen bonds. Three sets of complexes have been identified.

1. Conformation A complexes are stabilized by P···P σ–σ bonds. Of the three sets of complexes, the A conformers are the most weakly bound, with binding energies ranging from −3.1 to −7.4 kJ/mol. A conformers are stabilized by charge-transfer interactions, the more stabilizing of which arises from transfer of the P_t lone pair of P_tCH to the σ*P_s-A orbital of P_sH_2X, where A is the atom of X directly bonded to P. Charge transfer from the lone pair of P_s to the σ*P=C orbital is a less stabilizing interaction.
2. Conformation B and C complexes are stabilized by σ–π bonds, that is, bonds that involve interaction between the σ system of PH_2X and the π system of PCH. In both sets of conformers, the preferred direction of charge transfer is from the π bond of PCH through the σ-hole to the σ*P–A orbital of PH_2X and secondarily from the lone pair on P_s through the π-hole to the π*P=C orbital.
3. Conformation B and C complexes have similar binding energies, which range from −7.5 to −17.6 kJ/mol. They are differentiated structurally in so far as B complexes have A-P_s···C approaching linearity, whereas C complexes have A-P_s···P_t approaching linearity.

4. The binding energies of conformation A, B, and C complexes do not correlate with the intermolecular P–P distances. However, the dominant charge-transfer energies in each set do correlate with the intermolecular P–P distance.
5. EOM-CCSD ^{31}P–^{31}P spin–spin coupling constants $^{1p}J(P–P)$ correlate with the P–P distances in conformations A, B, and C. The largest coupling constants are found for conformation A complexes, a result of the nature of the σ–σ pnicogen bond and the dominance of the Fermi contact term. For a given substituent X, the ordering of $^{1p}J(P–P)$ is A > C > B >.

Acknowledgments This work was carried out with financial support from the Ministerio de Educación y Ciencia (Project No. CTQ2012-35513-C02-02) and Comunidad Autónoma de Madrid (Project MADRISOLAR2, ref S2009/PPQ1533). Thanks are given to the Ohio Supercomputer Center for its continued support and to the CTI (CSIC). This paper is dedicated in memory of Shi Shavitt, mentor, colleague, and friend.

References

1. Zahn S, Frank R, Hey-Hawkins E, Kirchner B (2011) Pnicogen bonds: a new molecular linker? Chem Eur J 17:6034–6038
2. Solimannejad M, Gharabaghi M, Scheiner S (2011) SH···N and SH···P blue-shifting H-bonds and N···P interactions in complexes pairing HSN with amines and phosphines. J Chem Phys 134(1–6):024312
3. Scheiner SA (2011) New noncovalent force: comparison of P···N interaction with hydrogen and halogen bonds. J Chem Phys 134(1–9):094315
4. Scheiner S (2011) Effects of substituents upon the P···N noncovalent interaction: the limits of its strength. J Phys Chem A 115:11202–11209
5. Adhikari U, Scheiner S (2012) Substituent effects on Cl···N, S···N and P···N noncovalent bonds. J Phys Chem A 116:3487–3497
6. Adhikari U, Scheiner S (2012) Sensitivity of pnicogen chalcogen halogen and H-bonds to angular distortions. Chem Phys Lett 532:31–35
7. Scheiner S (2011) Can two trivalent N atoms engage in a direct N···N noncovalent interaction? Chem Phys Lett 514:32–35
8. Scheiner S (2011) Effects of multiple substitution upon the P···N noncovalent interaction. Chem Phys 387:79–84
9. Scheiner S (2011) On the properties of X···N noncovalent interactions for first- second- and third-row x atoms. J Chem Phys 134(1–9):164313
10. Adhikari U, Scheiner S (2011) Comparison of P···D (D = P, N) with other noncovalent bonds in molecular aggregates. J Chem Phys 135(1–10):184306
11. Scheiner S, Adhikari U (2011) Abilities of different electron donors (d) to engage in a p d noncovalent interaction. J Phys Chem A 115:11101–11110
12. Scheiner S (2011) Weak H-bonds: comparisons of CH···O to NH···O in proteins and PH···N to direct P···N interactions. Phys Chem Chem Phys 13:13860–13872
13. Del Bene JE, Alkorta I, Sánchez-Sanz G, Elguero J (2011) ^{31}P-^{31}P spin–spin coupling constants for pnicogen homodimers. Chem Phys Lett 512:184–187
14. Del Bene JE, Alkorta I, Sánchez-Sanz G, Elguero J (2014) Structures, energies, bonding, and NMR properties of pnicogen complexes $H_2XP:NXH_2$ (X = H, CH_3, NH_2, OH, F, Cl). J Phys Chem A 115:13724–13731
15. Adhikari U, Scheiner S (2012) Effects of carbon chain substituents on the P···N noncovalent bond. Chem Phys Lett 536:30–33
16. Li Q-Z, Li R, Liu X-F, Li W-Z, Cheng J-B (2012) Pnicogen-hydride interaction between FH_2X (X = P and As) and HM (M = ZnH, BeH, MgH, Li and Na). J Phys Chem A 116:2547–2553
17. Li Q-Z, Li R, Liu X-F, Li W-Z, Cheng J-B (2012) Concerted interaction between pnicogen and halogen bonds in XCl-FH_2P-NH_3 (X = F, OH, CN, NC and FCC). ChemPhysChem 13:1205–1212
18. Del Bene JE, Alkorta I, Sánchez-Sanz G, Elguero J (2012) Structures, binding energies, and spin–spin coupling constants of geometric isomers of pnicogen homodimers $(PHFX)_2$ X = F, Cl, CN, CH_3, NC. J Phys Chem A 116:3056–3060
19. Del Bene JE, Alkorta I, Sánchez-Sanz G, Elguero J (2012) Homo- and heterochiral dimers $(PHFX)_2$ X = Cl, CN, CH_3, NC: To what extent do they differ? Chem Phys Lett 538:14–18
20. Alkorta I, Sánchez-Sanz G, Elguero J, Del Bene JE (2012) Influence of hydrogen bonds on the P···P pnicogen bond. J Chem Theor Comp 8:2320–2327
21. An X-L, Li R, Li Q-Z, Liu X-F, Li W-Z, Cheng J-B (2012) Substitution cooperative and solvent effects on π pnicogen bonds in the FH_2P and FH_2As Complexes. J Mol Model 18:4325–4332
22. Bauzá A, Quiñonero D, Deyà PM, Frontera A (2012) Pnicogen-π complexes: theoretical study and biological implications. Phys Chem Chem Phys 14:14061–14066
23. Alkorta I, Sánchez-Sanz G, Elguero J, Del Bene JE (2013) Exploring $(NH_2F)_2$, $H_2FP:NFH_2$ and $(PH_2F)_2$ potential surfaces: hydrogen bonds or pnicogen bonds? J Phys Chem A 117:183–191
24. Sánchez-Sanz G, Alkorta I, Elguero J (2013) Intramolecular pnicogen interactions in PHF-$(CH_2)_n$-PHF (n = 2–6) systems. ChemPhysChem 14:1656–1665
25. Del Bene JE, Alkorta I, Sánchez-Sanz G, Elguero J (2013) Phosphorus as a simultaneous electron-pair acceptor in intermolecular P···N pnicogen bonds and electron-pair donor to Lewis acids. J Phys Chem A 117:3133–3141
26. Grabowski SJ, Alkorta I, Elguero J (2013) Complexes between dihydrogen and amine phosphine and arsine derivatives: hydrogen bond versus pnictogen interaction. J Phys Chem A 117:3243–3325
27. Politzer P, Murray J, Clark T (2013) Halogen bonding and other σ-hole interactions: a perspective. Phys Chem Chem Phys 15:11178–11189
28. Alkorta I, Elguero J, Del Bene JE (2013) Pnicogen-bonded cyclic trimers $(PH_2X)_3$ with X = F, Cl, OH, NC, CN, CH_3, H and BH_2. J Phys Chem A 117:4981–4987
29. Sánchez-Sanz G, Trujillo C, Solimannejad M, Alkorta I, Elguero J (2013) Orthogonal interactions between nitryl derivatives and electron donors: pnictogen bonds. Phys Chem Chem Phys 15:14310–14318
30. Del Bene JE, Alkorta I, Elguero J (2013) Characterizing complexes with pnicogen bonds involving sp^2 hybridized phosphorus atoms: $(H_2C=PX)_2$ with X = F, Cl, OH, CN, NC, CCH, H, CH_3 and BH_2. J Phys Chem A 117:6893–6903
31. Alkorta I, Elguero J, Del Bene JE (2013) Pnicogen bonded complexes of PO_2X (X = F, Cl) with nitrogen bases. J Phys Chem A 117:10497–10503
32. Del Bene JE, Alkorta I, Elguero J (2013) Properties of complexes $H_2C=(X)P:PXH_2$ for X = F, Cl, OH, CN, NC, CCH, H, CH_3 and BH_2: P···P pnicogen bonding at σ-holes and π-holes. J Phys Chem A 117:11592–11604

33. Solimannejad M, Nassirinia N, Amani SA (2013) Computational study of 1:1 and 1:2 complexes of nitryl halides (O_2NX) with HCN and HNC. Struct Chem 24:651–659
34. Solimannejad M, Ramezani V, Trujillo C, Alkorta I, Sánchez-Sanz G, Elguero J (2012) Competition and interplay between σ-hole and π-hole interactions: a computational study of 1:1 and 1:2 complexes of nitryl halides (O_2NX) with ammonia. J Phys Chem A 116:5199–5206
35. Pople JA, Binkley JS, Seeger R (1976) Theoretical models incorporating electron correlation. Int J Quantum Chem Quantum Chem Symp 10:1–19
36. Krishnan R, Pople JA (1978) Approximate fourth-order perturbation theory of the electron correlation energy. Int J Quantum Chem 14:91–100
37. Bartlett RJ, Silver DM (1975) Many-body perturbation theory applied to electron pair correlation energies in closed-shell first-row diatomic hydrides. J Chem Phys 62:3258–3268
38. Bartlett RJ, Purvis GD (1978) Many-body perturbation theory coupled-pair many-electron theory and the importance of quadruple excitations for the correlation problem. Int J Quantum Chem 14:561–581
39. Del Bene JE (1993) Proton affinities of ammonia, water, and hydrogen fluoride and their anions: a quest for the basis-set limit using the Dunning augmented correlation-consistent basis sets. J Phys Chem 97:107–110
40. Dunning TH (1989) Gaussian basis sets for use in correlated molecular calculations: i. the atoms boron through neon and hydrogen. J Chem Phys 90:1007–1023
41. Woon DE, Dunning TH (1995) Gaussian basis sets for use in correlated molecular calculations: v. core-valence basis sets for boron through neon. J Chem Phys 103:4572–4585
42. Frisch MJ, Trucks GW, Schlegel HB, Scuseria GE, Robb MA, Cheeseman JR, Scalmani G, Barone V, Mennucci B, Petersson GA et al. Gaussian Inc: Wallingford CT 2009 Gaussian-09 Revision A01
43. Bader RFW (1991) A quantum theory of molecular structure and its applications. Chem Rev 91:893–928
44. Bader RFW (1990) Atoms in molecules a quantum theory. Oxford University Press, Oxford, England
45. Popelier PLA (2000) Atoms in molecules: an introduction. Prentice Hall, Harlow, England
46. Matta CF, Boyd RJ (2007) The quantum theory of atoms in molecules: from solid state to DNA and drug design. Wiley-VCH, Weinheim, Germany
47. Silvi B, Savin A (1994) Classification of chemical bonds based on topological analysis of electron localization functions. Nature 371:683
48. AIMAll (Version 110823) Todd A, Keith TK Gristmill Software Overland Park KS USA 2011. http://aim.tkgristmill.com. Accessed August 1 2013
49. Noury S, Krokidis X, Fuster F, Silvi B (1997) TopMod Package. Universite Pierre et Marie Curie, Paris, France
50. Reed AE, Curtiss LA, Weinhold F (1988) Intermolecular interactions from a natural bond orbital donor-acceptor viewpoint. Chem Rev 88:899–926
51. Glendening ED, Badenhoop JK, Reed AE, Carpenter JE, Bohmann JA, Morales CM, Landis CR, Weinhold F (2013) NBO 60. University of Wisconsin, Madison, WI
52. Perera SA, Nooijen M, Bartlett RJ (1996) Electron correlation effects on the theoretical calculation of nuclear magnetic resonance spin–spin coupling constants. J Chem Phys 104:3290–3305
53. Perera SA, Sekino H, Bartlett RJ (1994) Coupled-cluster calculations of indirect nuclear coupling constants: the importance of non-fermi contact contributions. J Chem Phys 101:2186–2196
54. Schäfer A, Horn H, Ahlrichs R (1992) Fully optimized contracted gaussian basis sets for atoms Li to Kr. J Chem Phys 97:2571–2577
55. Stanton JF, Gauss J, Watts JD, Nooijen M, Oliphant N, Perera SA, Szalay PS, Lauderdale WJ, Gwaltney SR, Beck S, et al. ACES II, University of Florida Gainesville, Fl